ADMX-Orpheus:
High-mass axion search with a dielectrically loaded Fabry-Perot interferometer

CPAD 2026

Seattle, WA

James Sinnis — Oct. 22, 2026

CENPA Center for Experimental Nuclear Physics and Astrophysics

UNIVERSITY of WASHINGTON



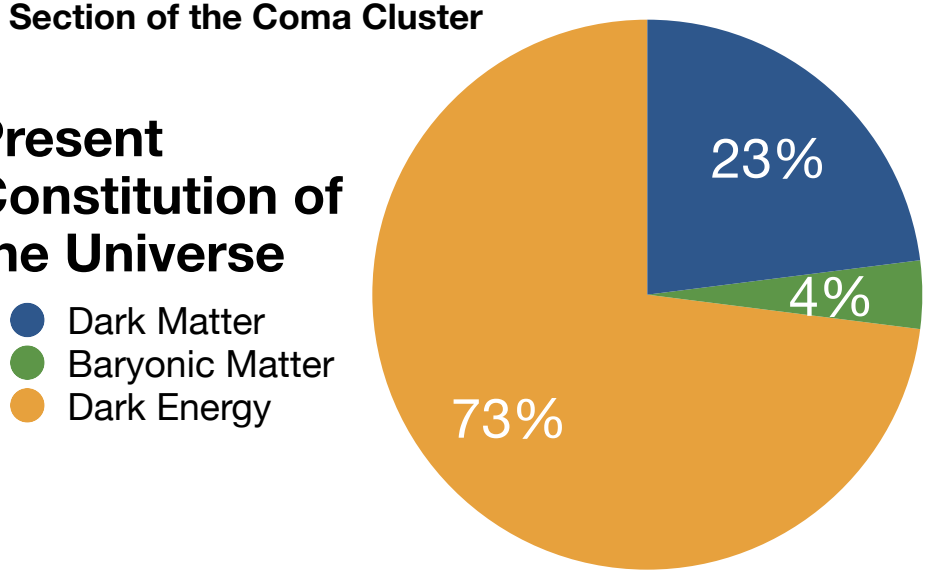
Dark Matter

- First observed in 1933
- Constitutes roughly 23% of the universe
- Is likely non-baryonic, outside of the standard model
- A necessary component of modern cosmology
- Has been observed for about 100 years



Section of the Coma Cluster

Present Constitution of the Universe

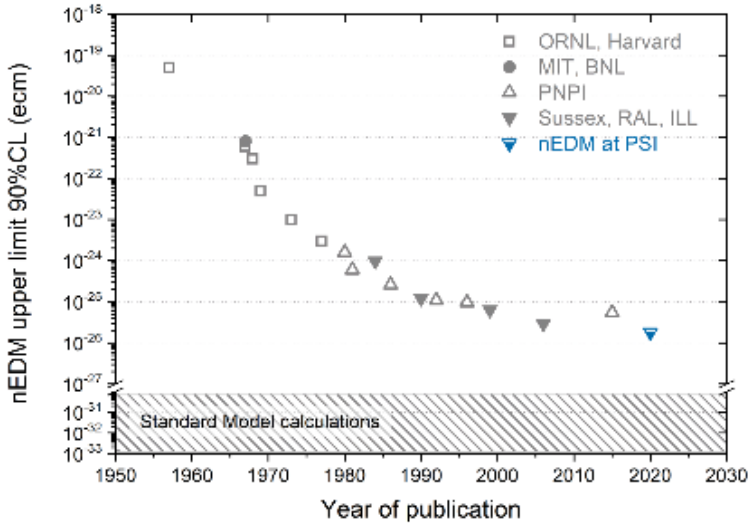


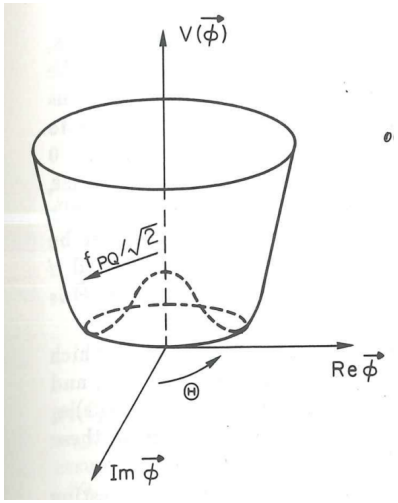
Axions as Dark Matter

- Neutron EDM measurements set $\theta < 10^{-11}$
- Multiple possible creation mechanisms, however…
- The misalignment mechanism produces a relation between the axion mass and the dark matter density
    - Prefers axion masses 1-100 μeV



$$\mathcal{L} \supset \theta \frac{g^2}{32\pi^2} F_{\mu\nu}\tilde{F}^{\mu\nu}$$





Misalignment Mechanism

Axion Detection — Modified Maxwell Equations

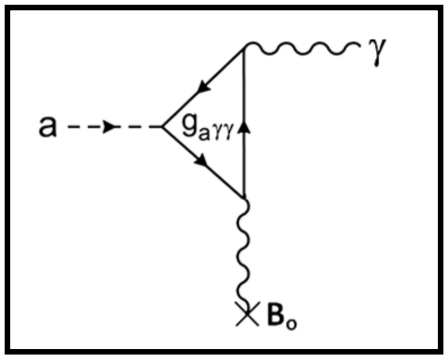
- Axions couple to the E and B fields
- Treat the dark matter halo as a background axion field
- This axion field mixes the magnetic and the electric fields
- A static magnetic field now produces an oscillating electric field

$$\nabla \cdot \boldsymbol{E} = -g_{a\gamma\gamma} \boldsymbol{B} \cdot \nabla a$$

$$\nabla \cdot \boldsymbol{B} = 0$$

$$\nabla \times \boldsymbol{E} = -\dot{\boldsymbol{B}}$$

$$\nabla \times \boldsymbol{B} = \dot{\boldsymbol{E}} + g_{a\gamma\gamma} \left(\dot{a} \boldsymbol{B} - \boldsymbol{E} \times \nabla a \right)$$



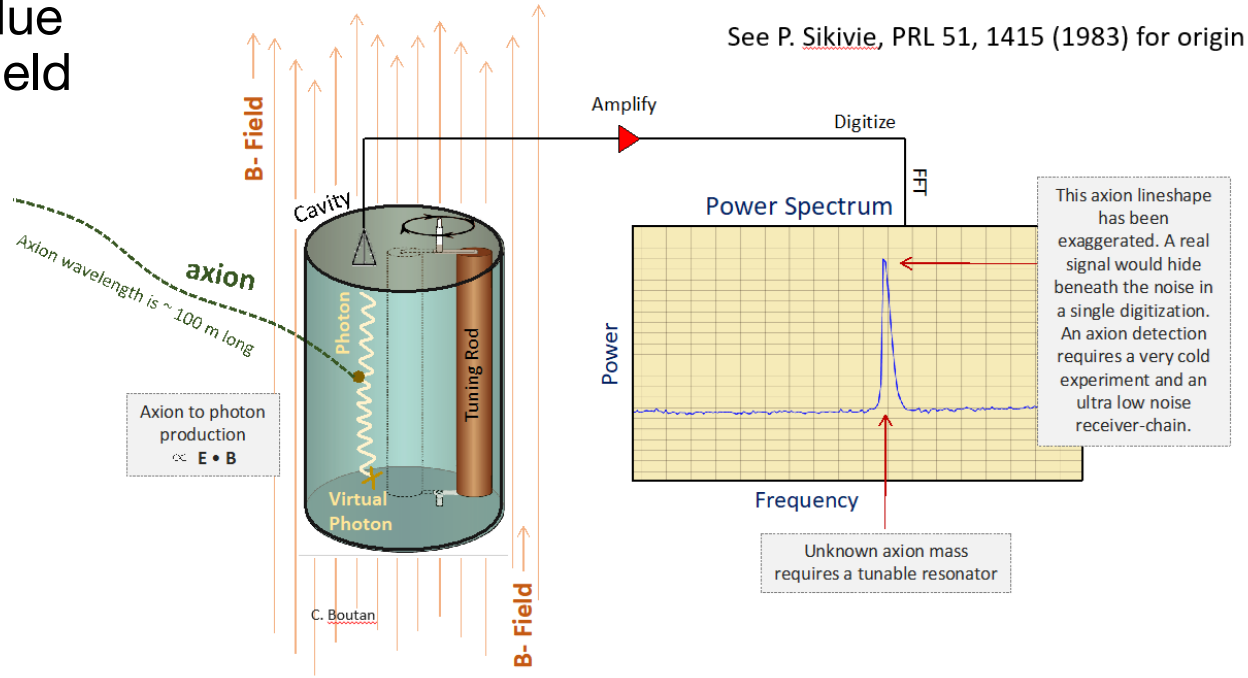
photon conversion

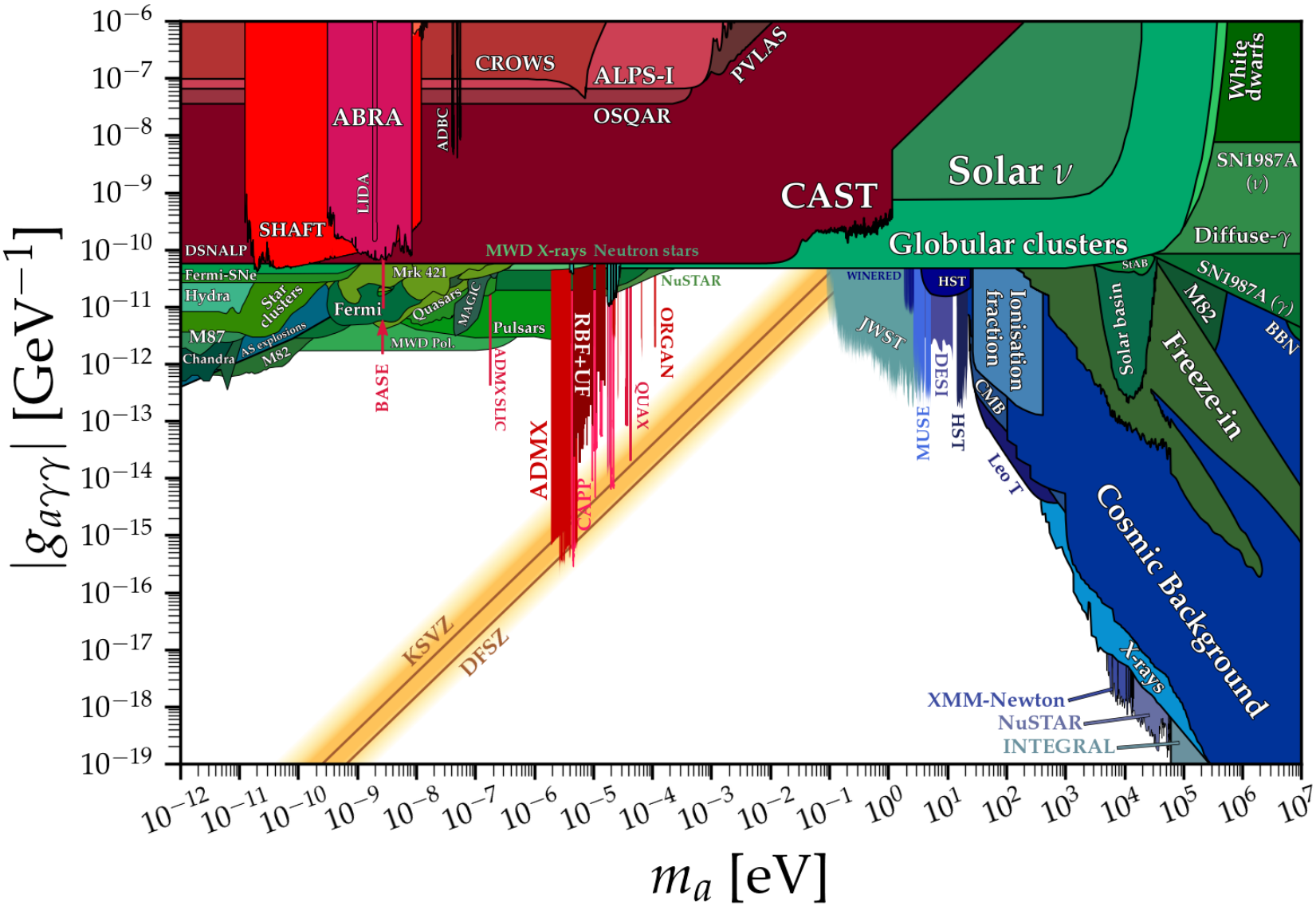
Axion Haloscopes

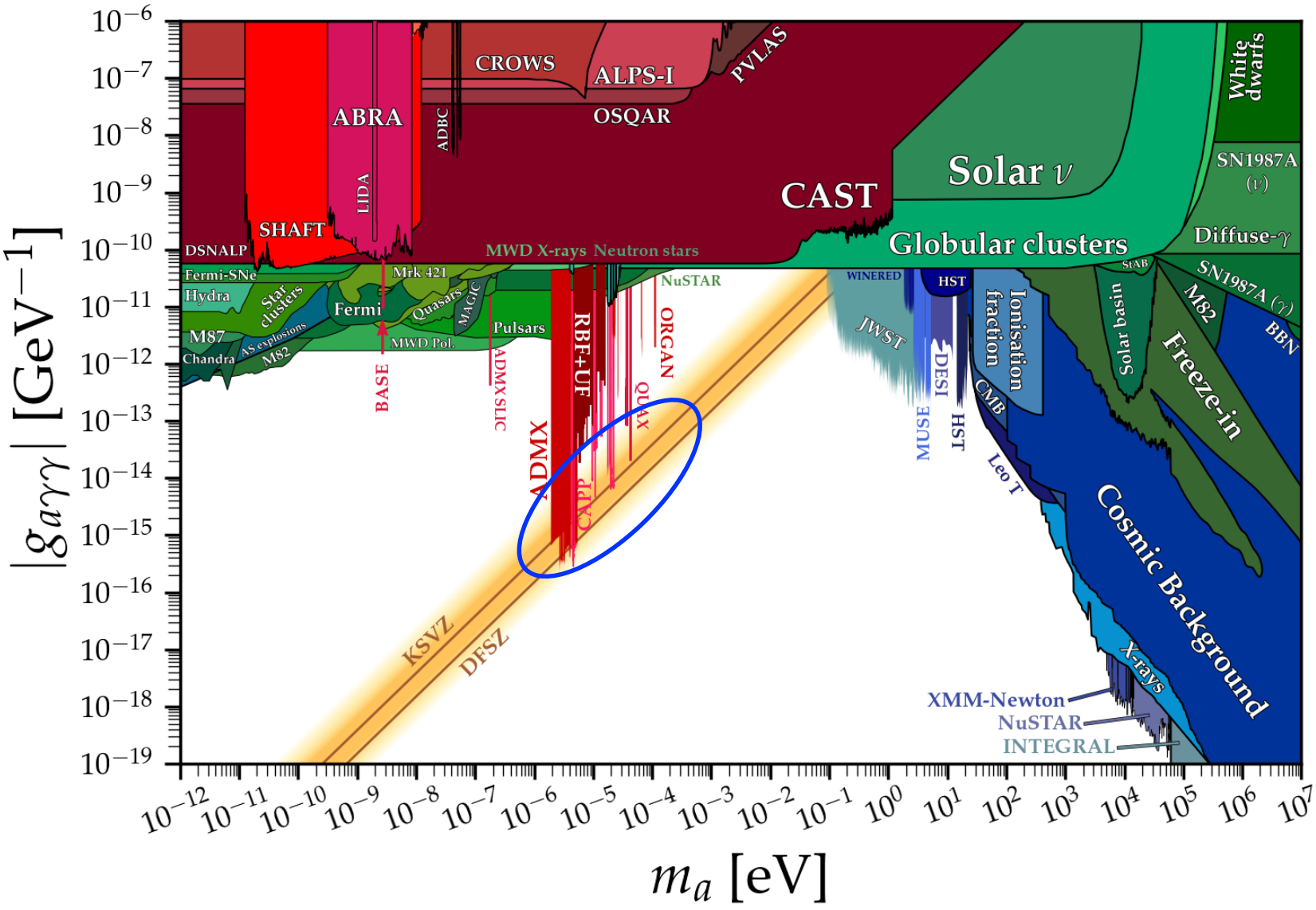
- External magnetic field $\boldsymbol{B_e}$
- Electric field oscillates at the axion Compton frequency due to oscillations in the axion field
- The resonant Cavity stores the energy of these oscillations.

$$\boldsymbol{E_a}(t) = -g_{a\gamma\gamma}a(t)\boldsymbol{B_e}$$

See P. Sikivie, PRL 51, 1415 (1983) for origin




$|g_{a\gamma\gamma}|$ [GeV^{-1}]
m_a [eV]
10^{-6}
10^{-7}
10^{-8}
10^{-9}
10^{-10}
10^{-11}
10^{-12}
10^{-13}
10^{-14}
10^{-15}
10^{-16}
10^{-17}
10^{-18}
10^{-19}
10^{-12} 10^{-11} 10^{-10} 10^{-9} 10^{-8} 10^{-7} 10^{-6} 10^{-5} 10^{-4} 10^{-3} 10^{-2} 10^{-1} 10^{0} 10^{1} 10^{2} 10^{3} 10^{4} 10^{5} 10^{6} 10^{7}
CROWS
ALPS-I
PVLAS
ABRA
ADBC
OSQAR
LIDA
CAST
Solar ν
White dwarfs
SN1987A (ν)
SHAFT
Globular clusters
Diffuse-γ
DSNALP
MWD X-rays
Neutron stars
Fermi-SNe
Hydra
Star clusters
Mrk 421
Fermi
Quasars
MAGIC
Pulsars
NuSTAR
WINERED
HST
StAB
SN1987A (γ)
M87
Chandra
AS explosions
M82
MWD Pol.
BASE
ADMX SLIC
RBF+UF
ORGAN
QUAX
ADMX
CAPP
JWST
DESI
MUSE
HST
Ionisation fraction
Solar basin
M82
Freeze-in
BBN
CMB
Leo T
Cosmic Background
X-rays
XMM-Newton
NuSTAR
INTEGRAL
KSVZ
DFSZ

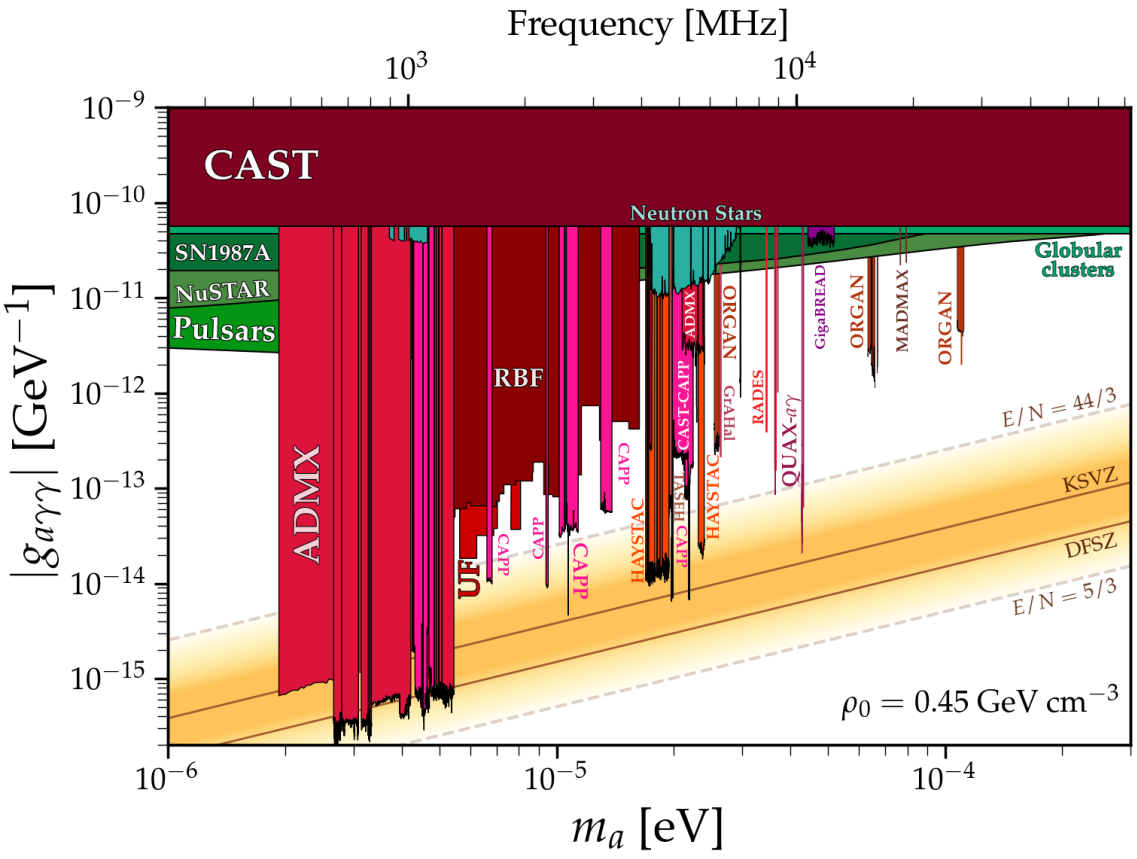

$|g_{a\gamma\gamma}|$ [GeV^{-1}]
m_a [eV]
10^{-6}
10^{-7}
10^{-8}
10^{-9}
10^{-10}
10^{-11}
10^{-12}
10^{-13}
10^{-14}
10^{-15}
10^{-16}
10^{-17}
10^{-18}
10^{-19}
10^{-12} 10^{-11} 10^{-10} 10^{-9} 10^{-8} 10^{-7} 10^{-6} 10^{-5} 10^{-4} 10^{-3} 10^{-2} 10^{-1} 10^{0} 10^{1} 10^{2} 10^{3} 10^{4} 10^{5} 10^{6} 10^{7}
CROWS
ALPS-I
PVLAS
ABRA
ADBC
OSQAR
LIDA
CAST
Solar ν
White dwarfs
SN1987A (ν)
SHAFT
Globular clusters
Diffuse-γ
DSNALP
MWD X-rays
Neutron stars
Fermi-SNe
Hydra
Star clusters
Mrk 421
Fermi
Quasars
MAGIC
NuSTAR
WINERED
HST
StAB
SN1987A (γ)
M87
Chandra
AS explosions
M82
MWD Pol.
Pulsars
BASE
ADMX SLIC
RBF+UF
ORGAN
QUAX
CAPP
ADMX
JWST
DESI
MUSE
HST
Ionisation fraction
Solar basin
M82
Freeze-in
BBN
CMB
Leo T
Cosmic Background
X-rays
XMM-Newton
NuSTAR
INTEGRAL
KSVZ
DFSZ

Resonant Cavity Design — Frequency Limitation

- Higher frequencies are limited by cavity volume
- Coupling to higher order modes is suppressed by the effective volume:

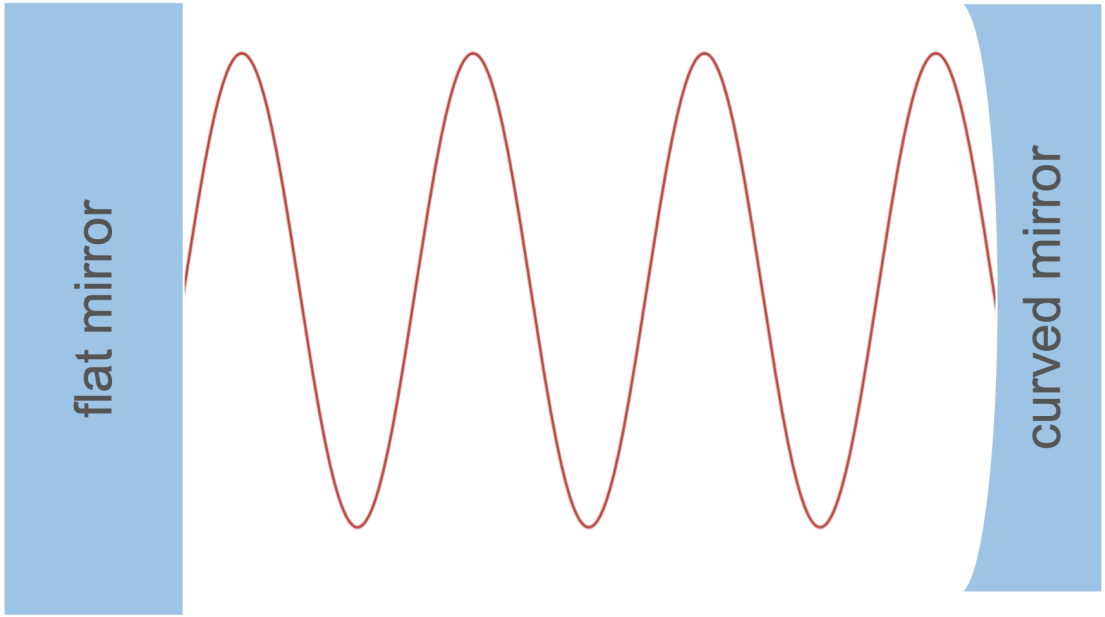
$$V_{\text{eff}} \propto \left| \int \vec{E}(\vec{x}) \cdot \vec{B}_{\text{ext}} d^3x \right|^2$$

- This is the motivation for new cavity designs

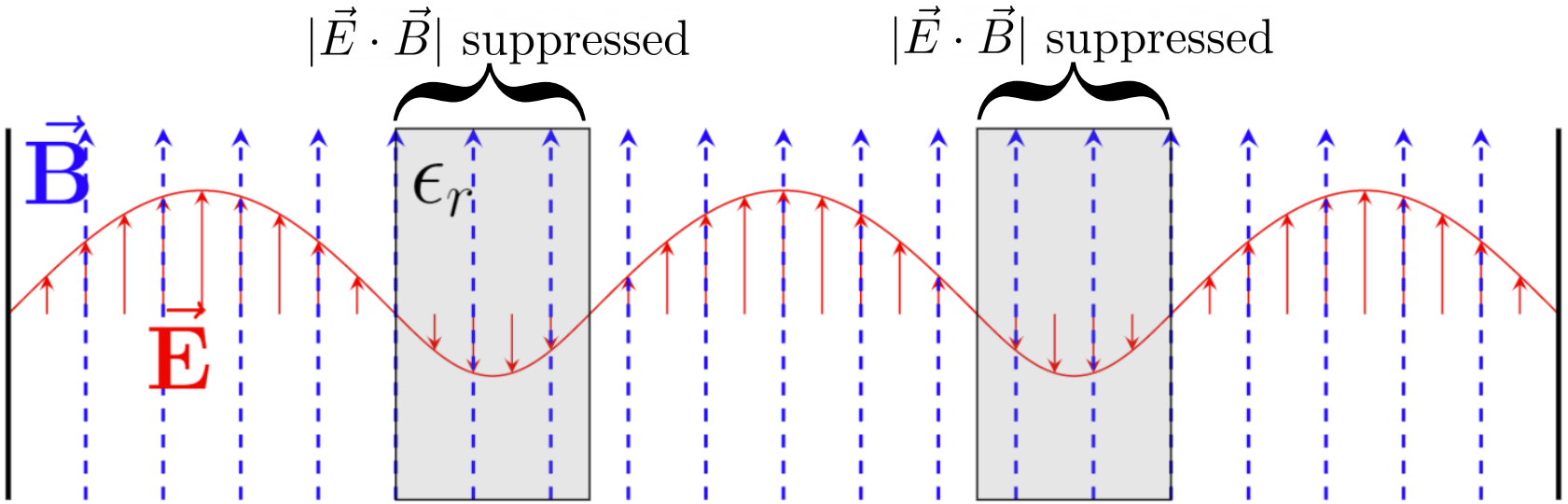


Fabry-Perot Interferometer as a Resonant Cavity

- TEM Standing Waves between two mirrors

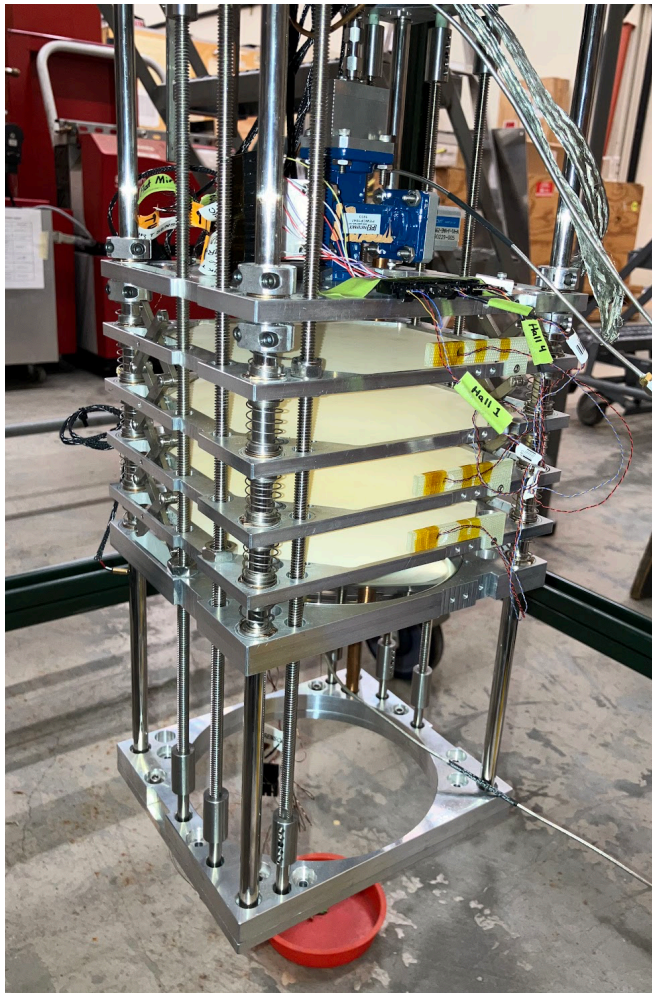


Dielectrics allow us to couple to higher order modes



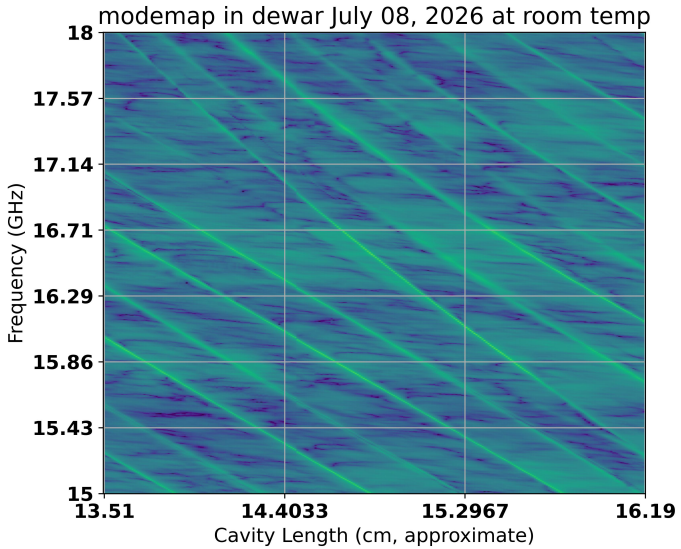
The Orpheus Resonator

- Built by Raphael Cervantes (FNAL)
- Coupling with the 18th order mode
- ~1 GHz bandwidth with 3mm thick dielectric plates
- Tuning range can be expanded by replacing dielectric plates



Resonator Tuning

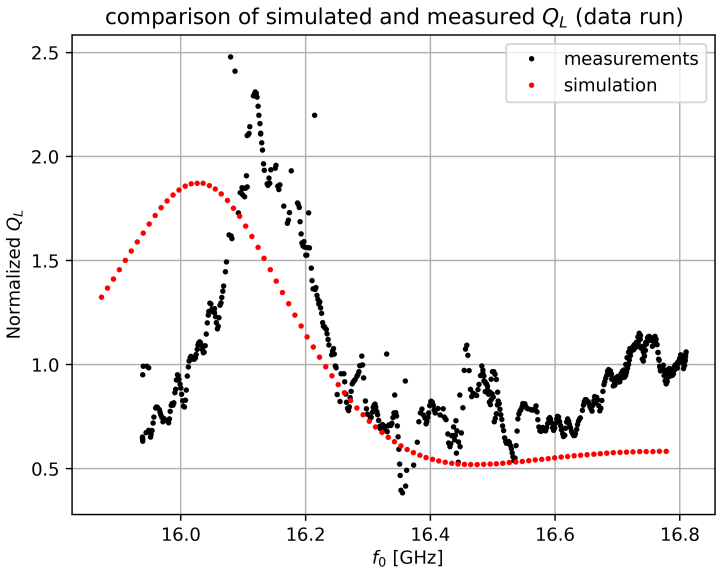
- The resonator needs to be tuned to conduct a scientifically interesting axion search.
- Three room temperature motors control three independent degrees of freedom in the cold space.
- The Fabry-Perot resonator has very few mode-crossings.

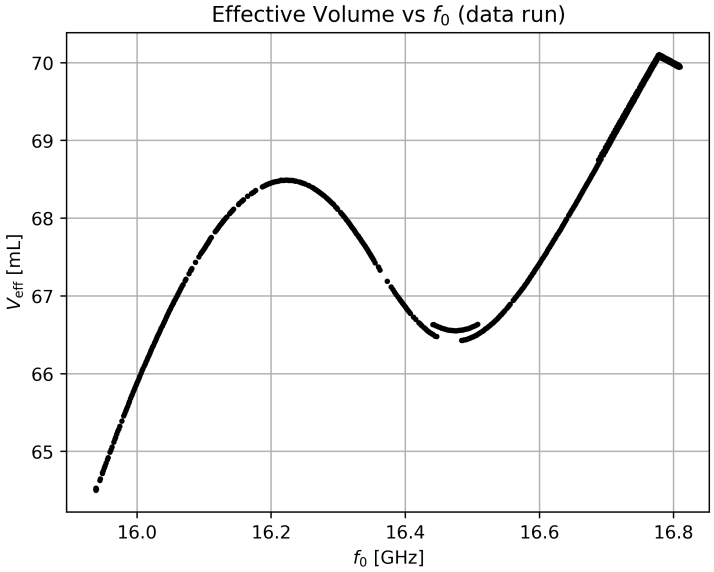


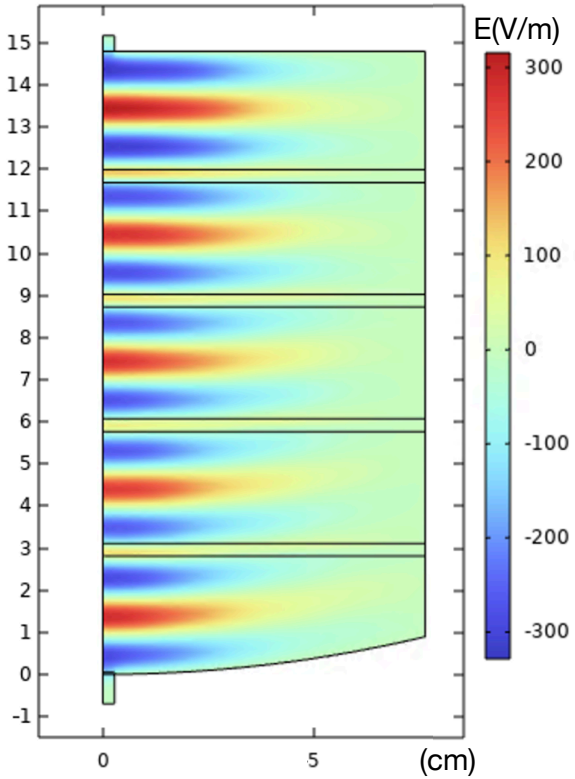


Cavity Simulations

- Our Effective Volume is approximated with simulations
- The effective volume is roughly 67 mL, we could double this by adding more plates
- ~10x increase in effective volume at this frequency, compared to closed cylindrical cavity

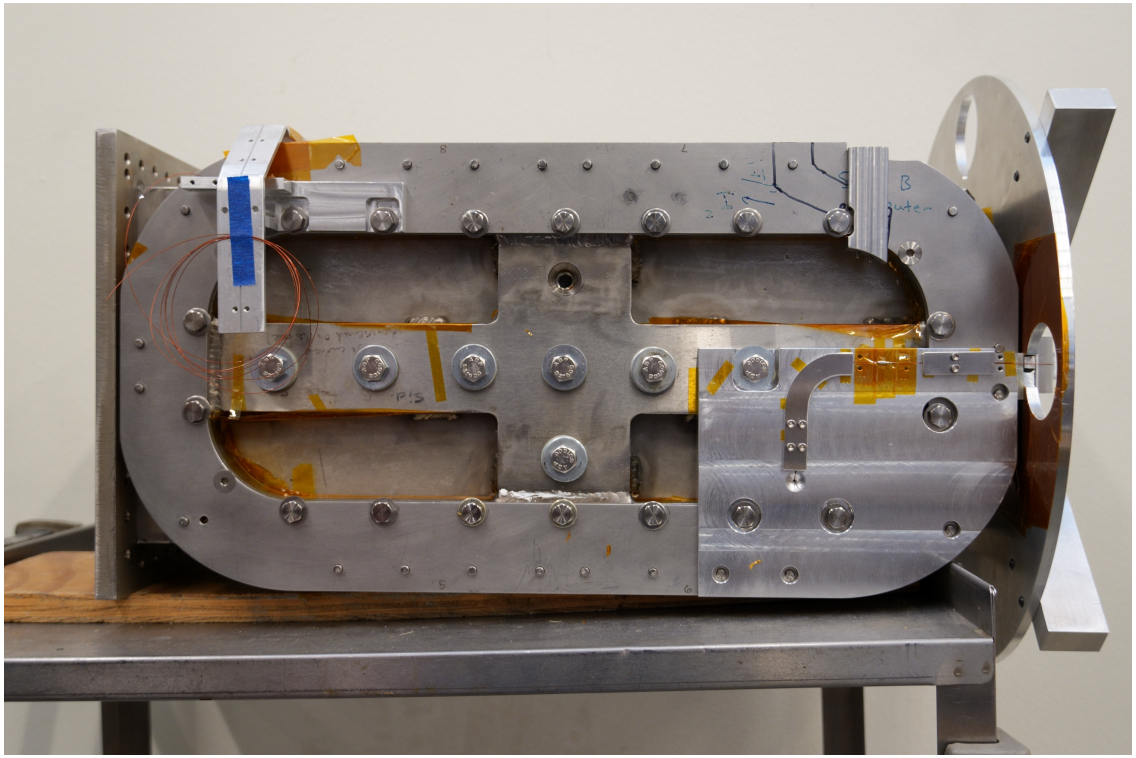






Orpheus Magnet

- Two-Coil Dipole Magnet
- Max field of ~0.50 Tesla
- Was damaged last year in a quench
- Should have a max field of about 1.0 Tesla
- Was wound and potted by hand at CENPA

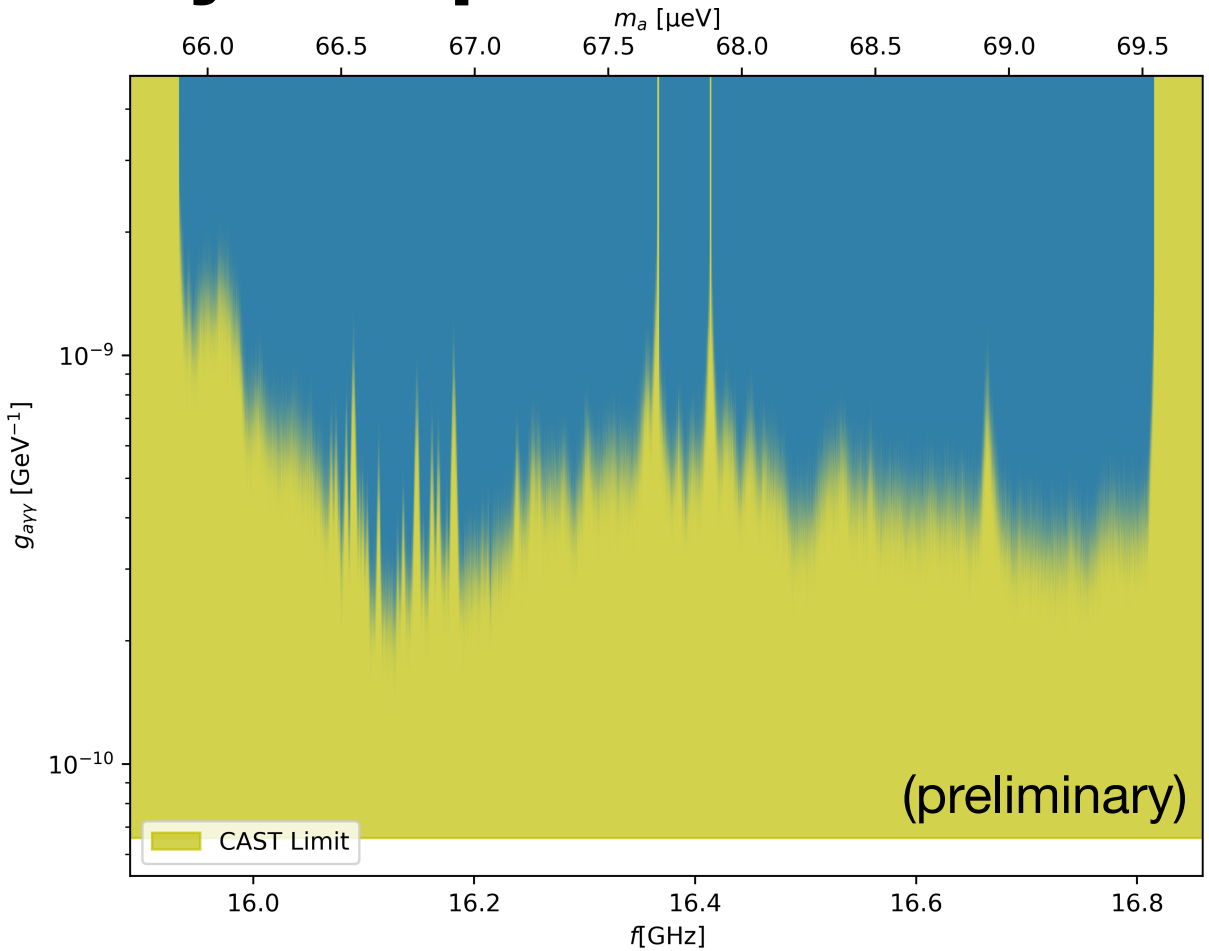


Data Taking (August)

- We ran with a low field, about 0.25 Tesla
- Cooled with Liquid Helium to 4.2 K
- Problem with digitizer drastically reduced our effective integration time
- Tuning system worked well



We are nearly competitive with solar limits



But both are far from the QCD axion at this mass…

But there are many improvements to make

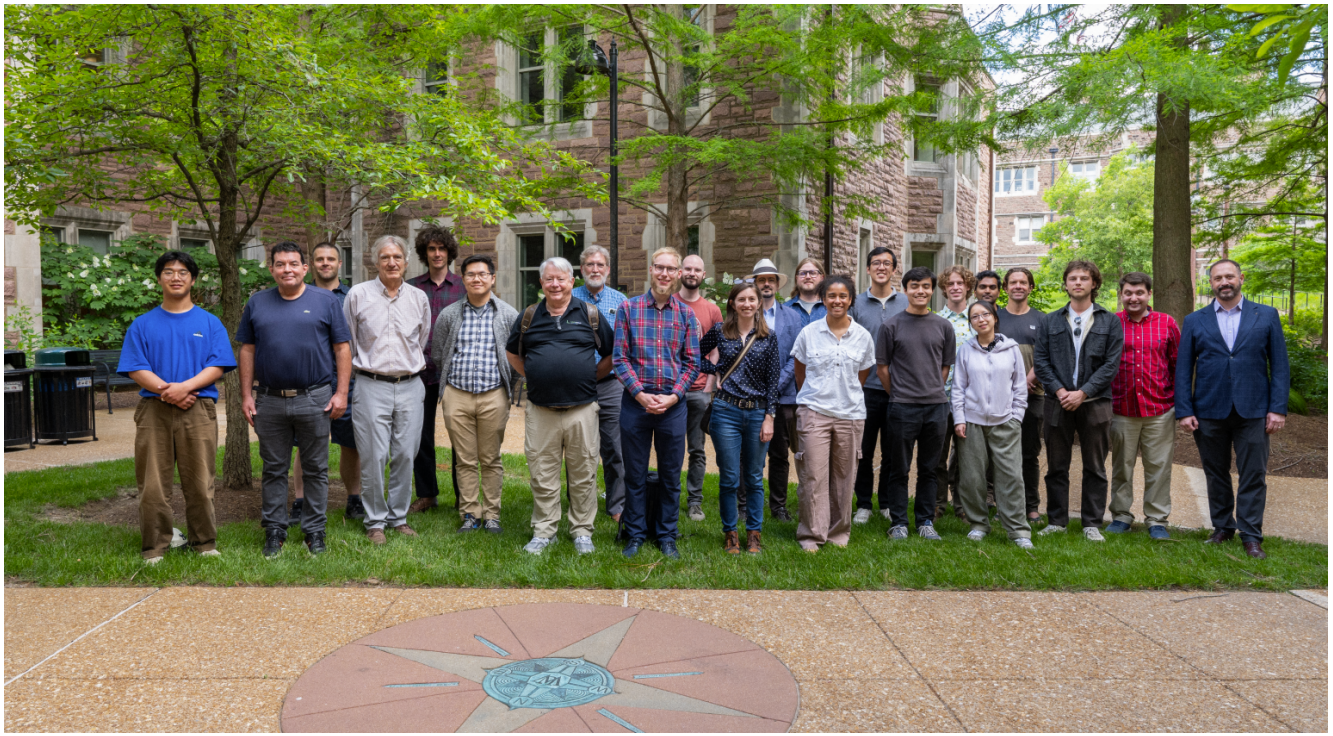
- Existing technology allows for:
  - ~20x reduction of noise temperature
  - Greater than ~2x improvement of effective volume
  - ~10x improvement of magnetic field strength
  - ~1000x increase in integration time
- This leads to a ~2 order of magnitude increase in sensitivity:

$$g_{a\gamma\gamma} = \frac{1}{B_0}\sqrt{\frac{\beta+1}{\beta}\frac{\mathrm{SNR}\times\Delta f T_n m_a}{\rho_a V_{eff} Q_L}}\left(\frac{1}{\Delta f t}\right)^{1/4}$$

In Conclusion

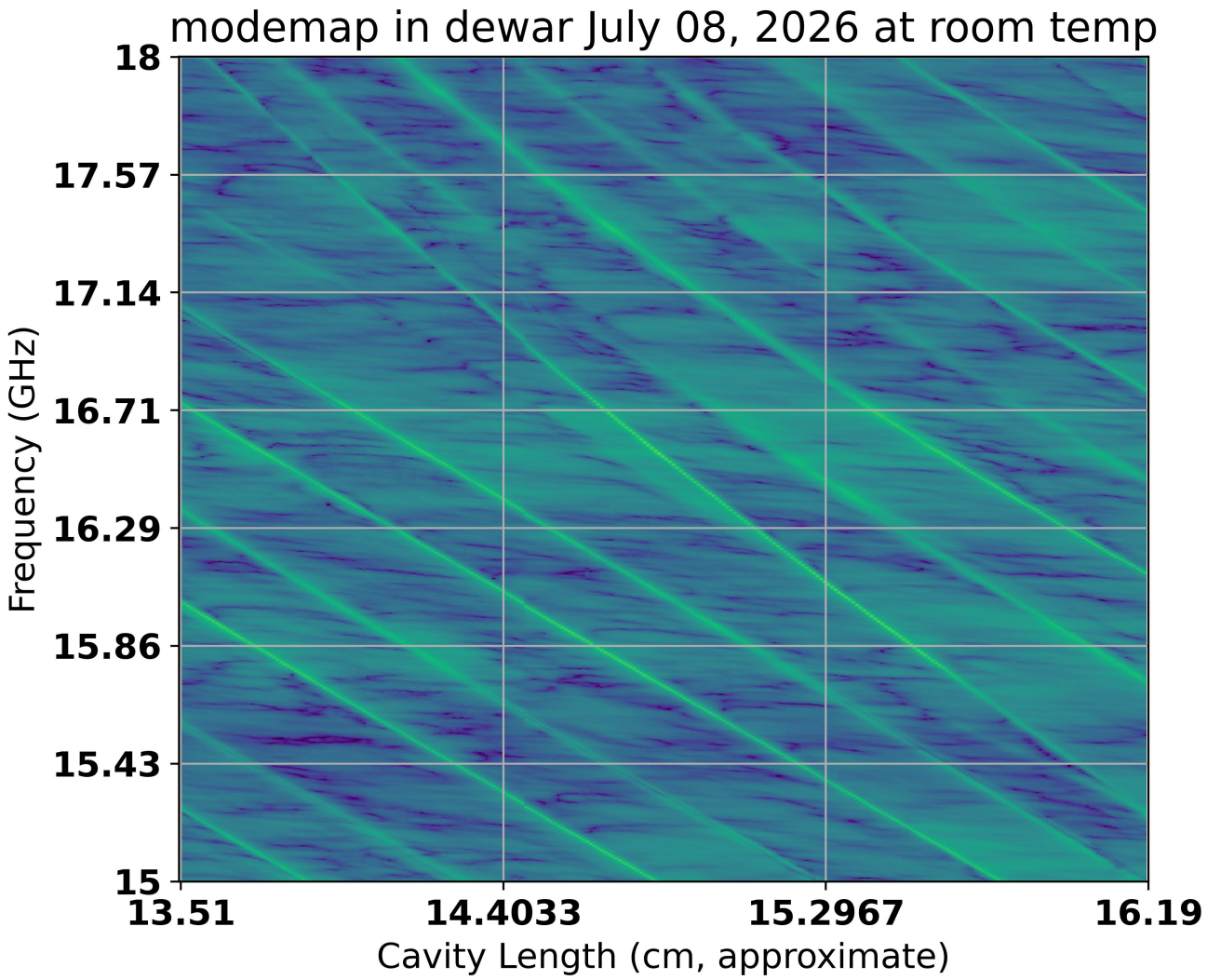
- Orpheus is an axion haloscope using dielectrics to couple to higher order modes of a resonator
- Orpheus has distinct advantages as an axion haloscope design:
    - Robust tuning mechanism without mode-crossings
    - Increased Effective Volume
    - Low-cost resonator that is not sensitive to perturbations
- Orpheus has a lot of obvious room for improvement, but scaling it to QCD axion sensitivity will require more research.
    - Less obvious improvements (coupling, mirror geometry)
    - Magnetic field strength (dipole magnets with fields >2 Tesla)
    - Using multiple cavities

Acknowledgements

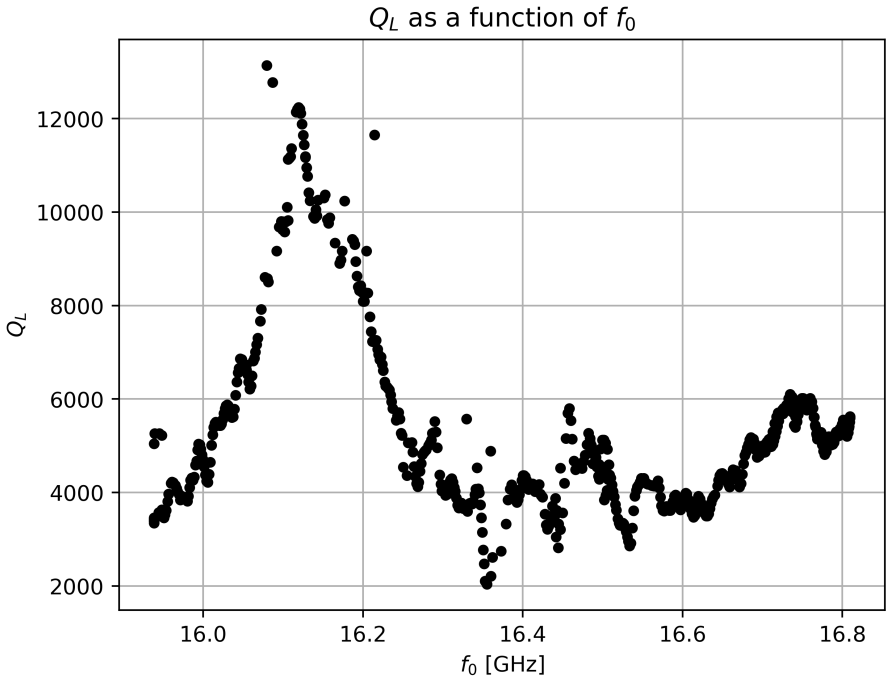


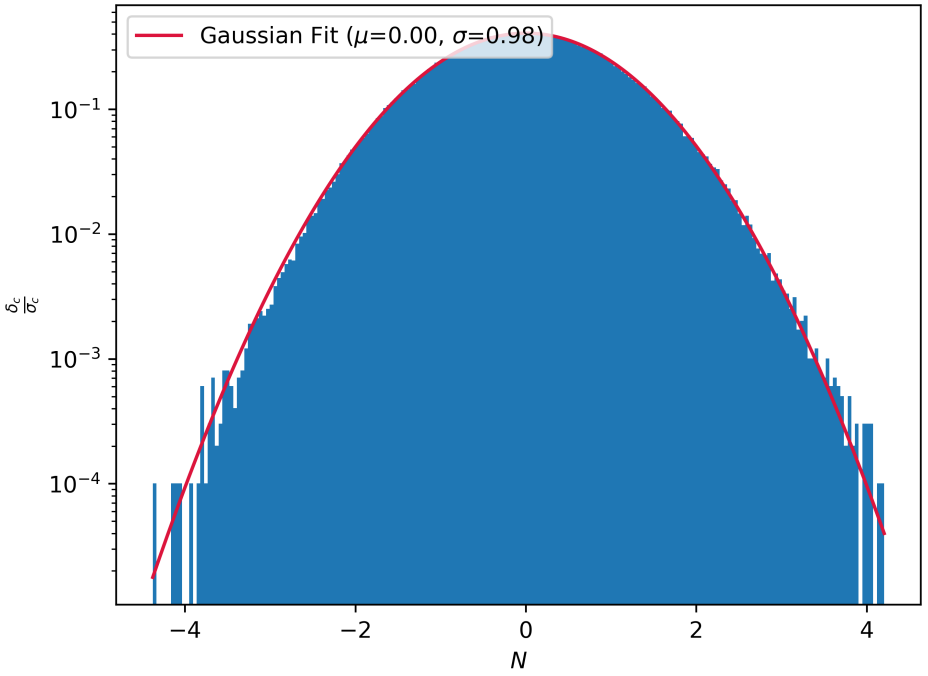
This work is supported by U.S. Department of Energy through Awards No DE-SC0009800, No. DE-SC0009723, No. DE-SC0010296, No. DE-SC0010280, No. DE-SC0011665, No. DEFG02-97ER41029, No. DE-FG02-96ER40956, No. DE-AC52-07NA27344, No. DE-C03-76SF00098, No. DE-SC-0022148 and No. DE-SC0017987. Fermilab is a U.S. Department of Energy, Office of Science, HEP User Facility managed by Fermi Research Alliance, LLC (FRA), under Contract No. DE-AC02-07CH11359. Additional support was provided by the Heising-Simons Foundation and by the Lawrence Livermore National Laboratory LDRD office. PNNL is a multi-program national laboratory operated for the U.S. DOE by Battelle Memorial Institute under Contract No. DE-AC05-76RL01830. UWA and Swinburne participation is funded by the ARC Centre of Excellence for Engineered Quantum Systems and CE170100009, Dark Matter Particle Physics, CE200100008. The Sheffield group acknowledges support from the UK Science and Technology Facilities Council (STFC) under grants ST/ T006811/1 and ST/X005879/1. CRB is supported by DOE Office of Science, High Energy Physics, Early Career Award (FWP 77794 at PNNL). Chelsea Bartram acknowledges support from the Panofsky Fellowship at SLAC. John Clarke acknowledges support from the U.S. Department of Energy, Office of Science, National Quantum Information Science Research Centers.

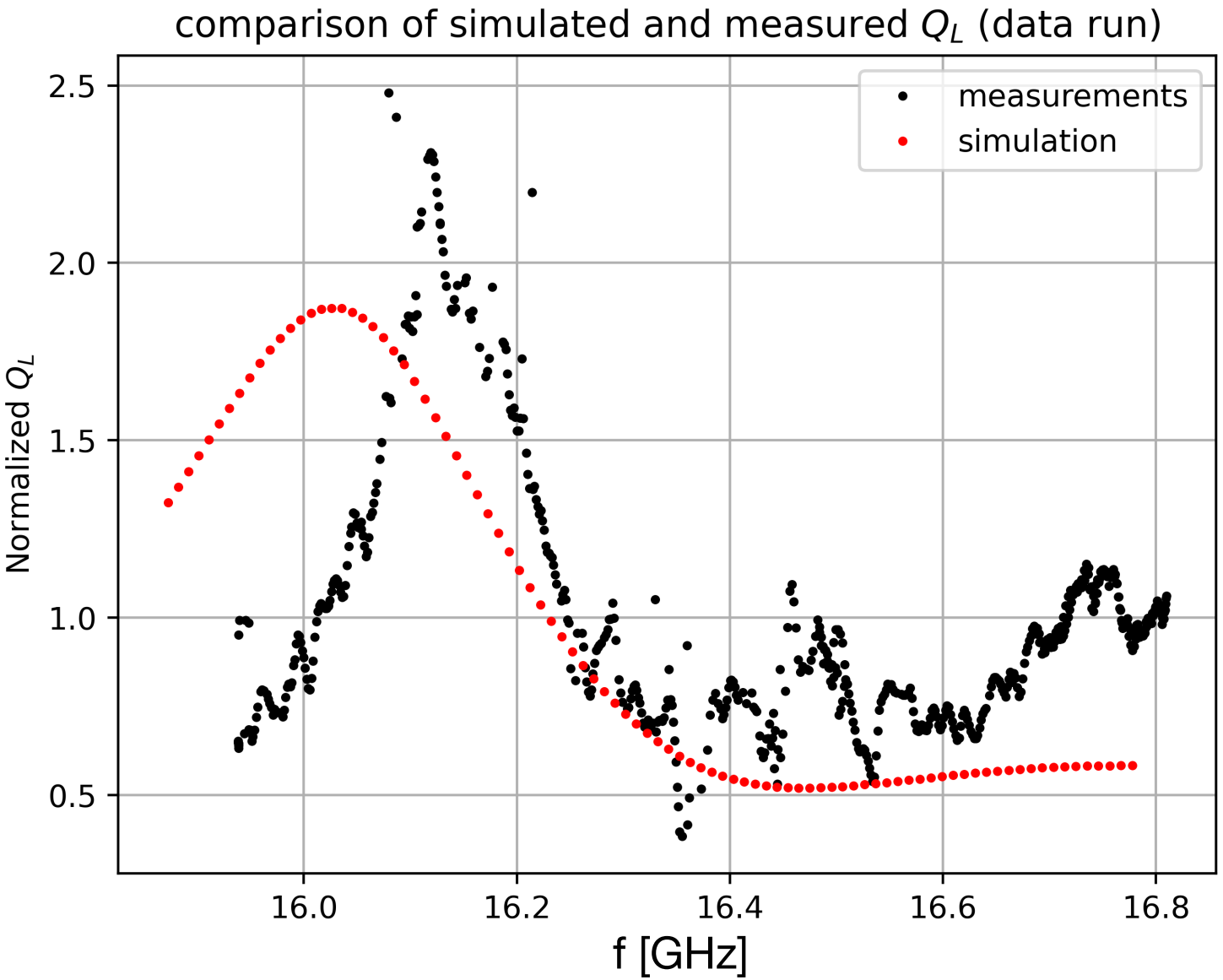
End

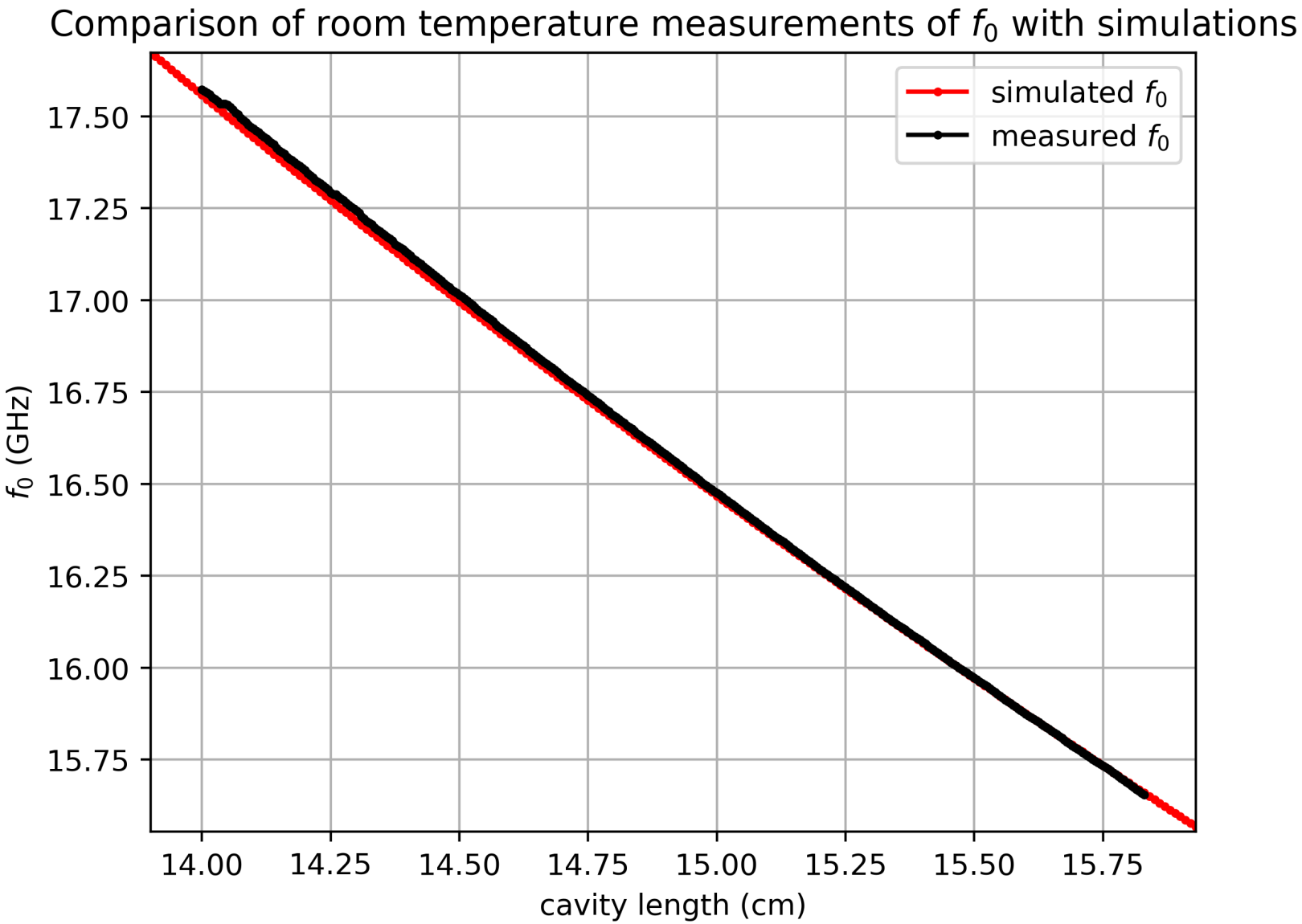

modemap in dewar July 08, 2026 at room temp
18
17.57
17.14
16.71
16.29
15.86
15.43
15
Frequency (GHz)
13.51
14.4033
15.2967
16.19
Cavity Length (cm, approximate)

Data Taking (August)



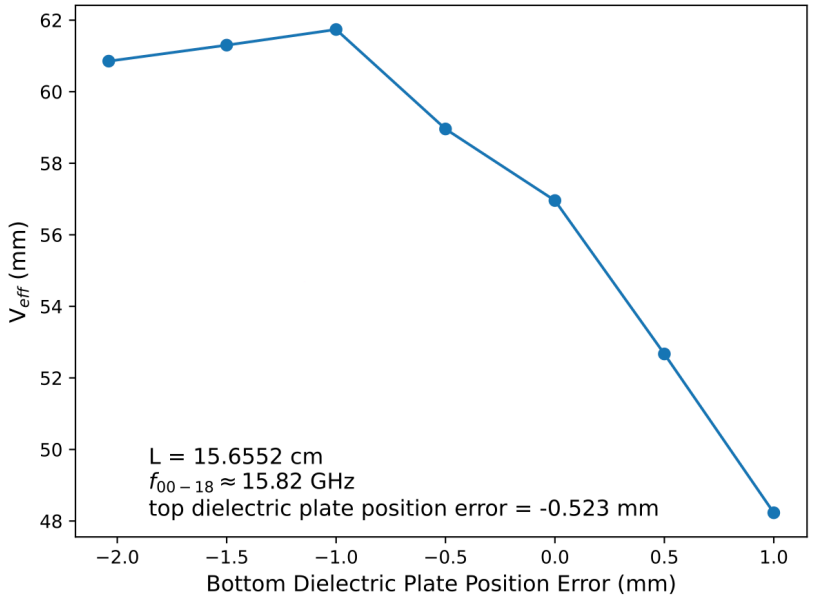


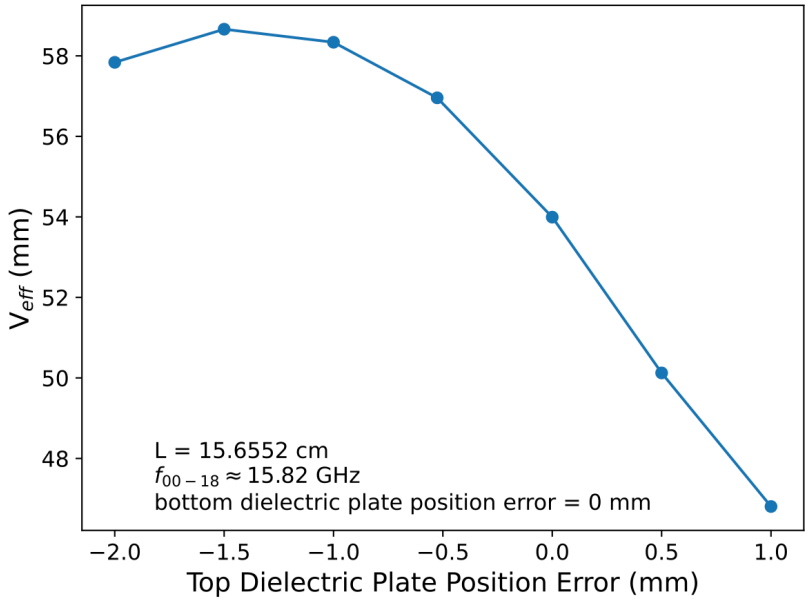

comparison of simulated and measured Q_L (data run)
measurements
simulation
Normalized Q_L
2.5
2.0
1.5
1.0
0.5
16.0
16.2
16.4
16.6
16.8
f [GHz]

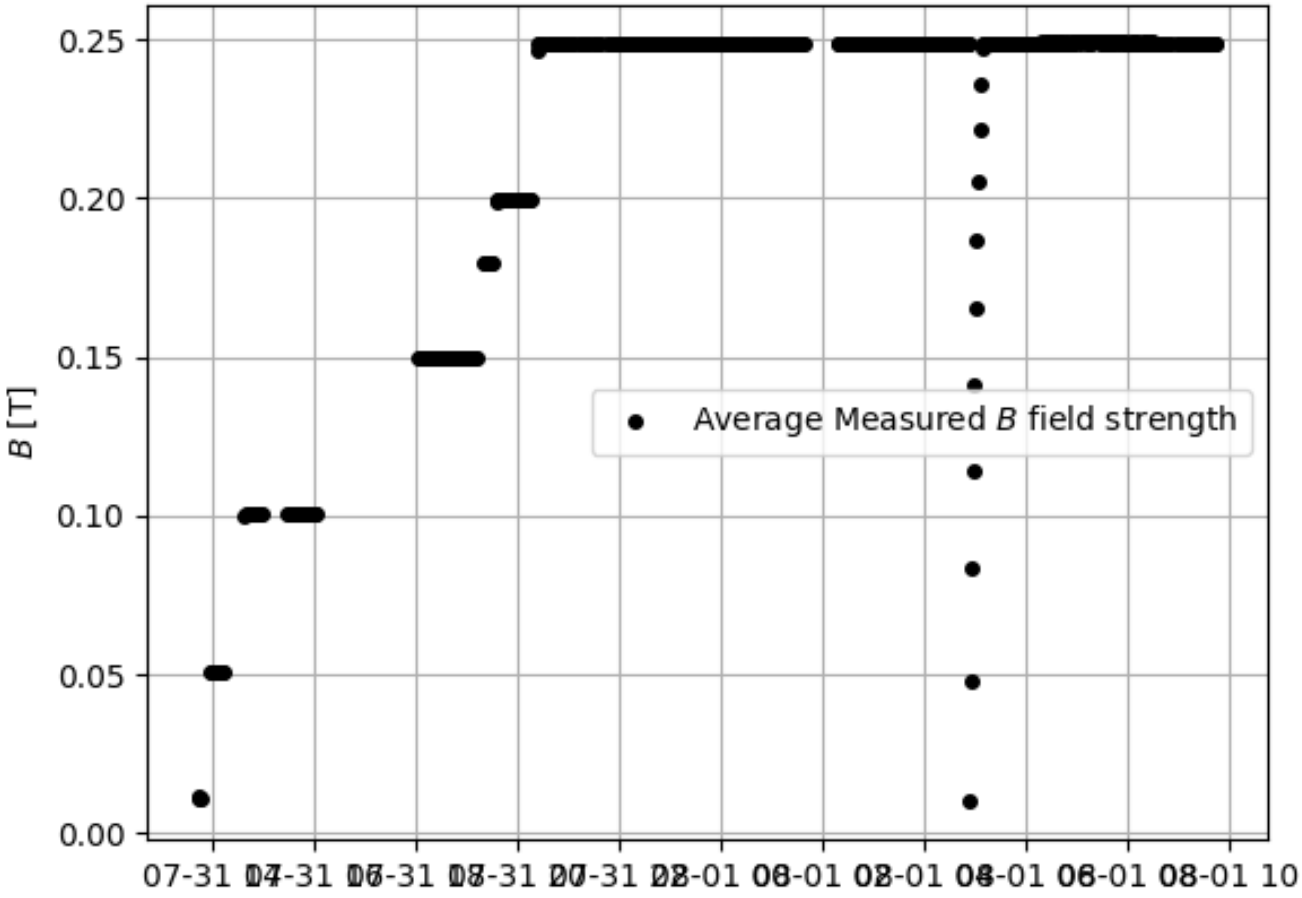

Comparison of room temperature measurements of f_0 with simulations
simulated f_0
measured f_0
17.50
17.25
17.00
16.75
16.50
16.25
16.00
15.75
f_0 (GHz)
14.00
14.25
14.50
14.75
15.00
15.25
15.50
15.75
cavity length (cm)

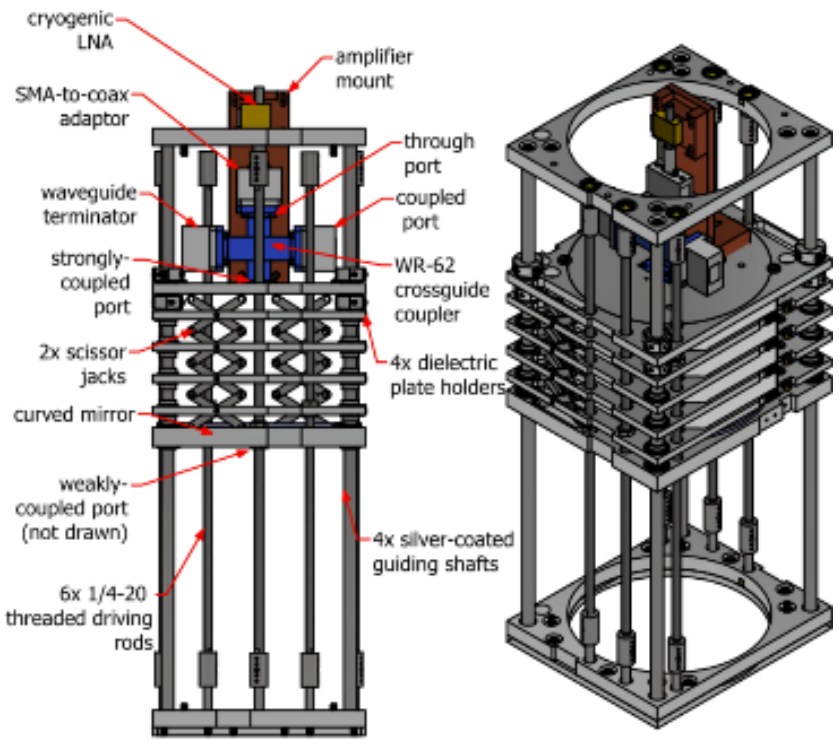
Sensitivity to dielectric position error

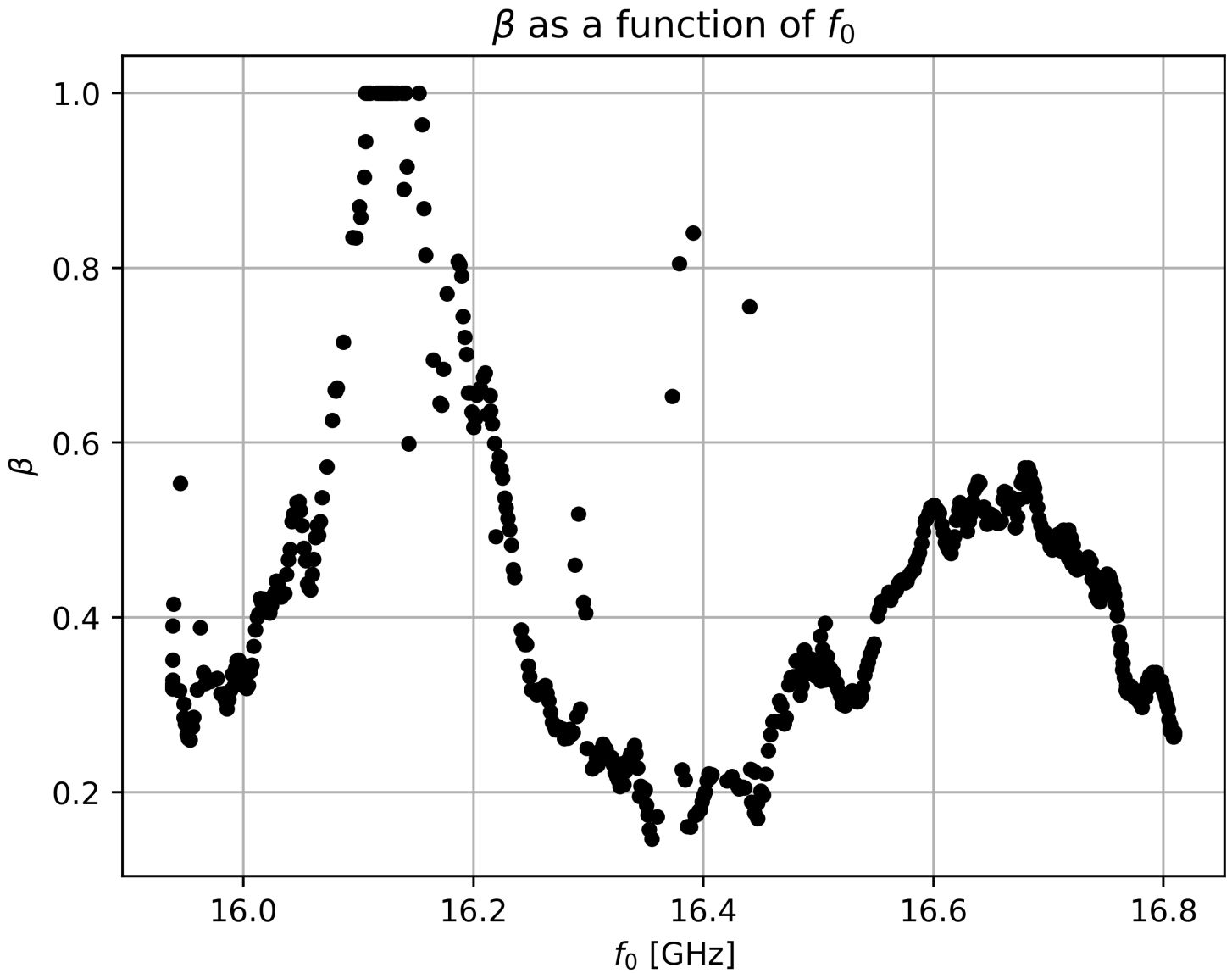
- Simulations show at most about a 7% reduction in effective volume per milliimeter displacement of the dielectric plates
- Precision of the motion system is about 0.2 millimeters.

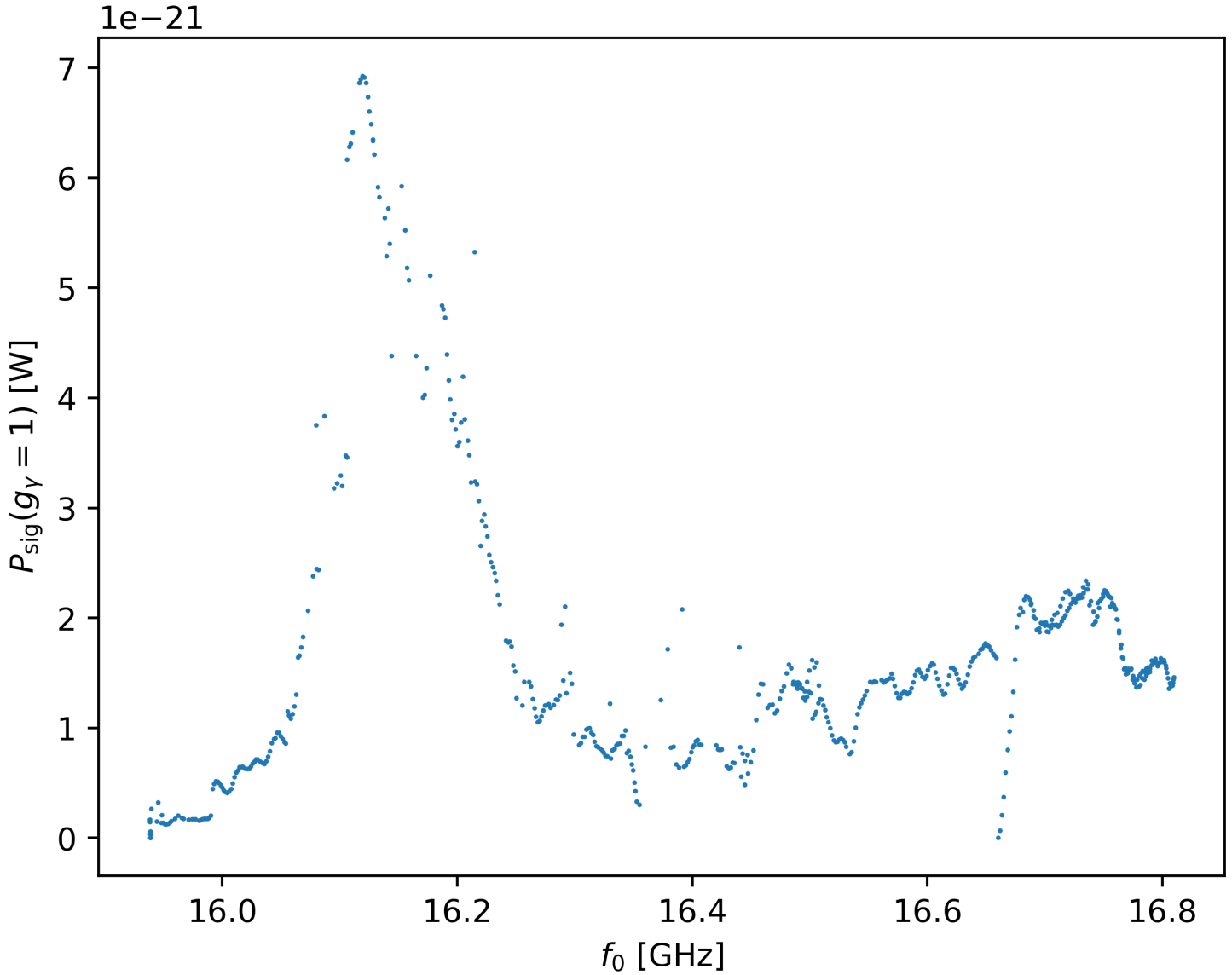


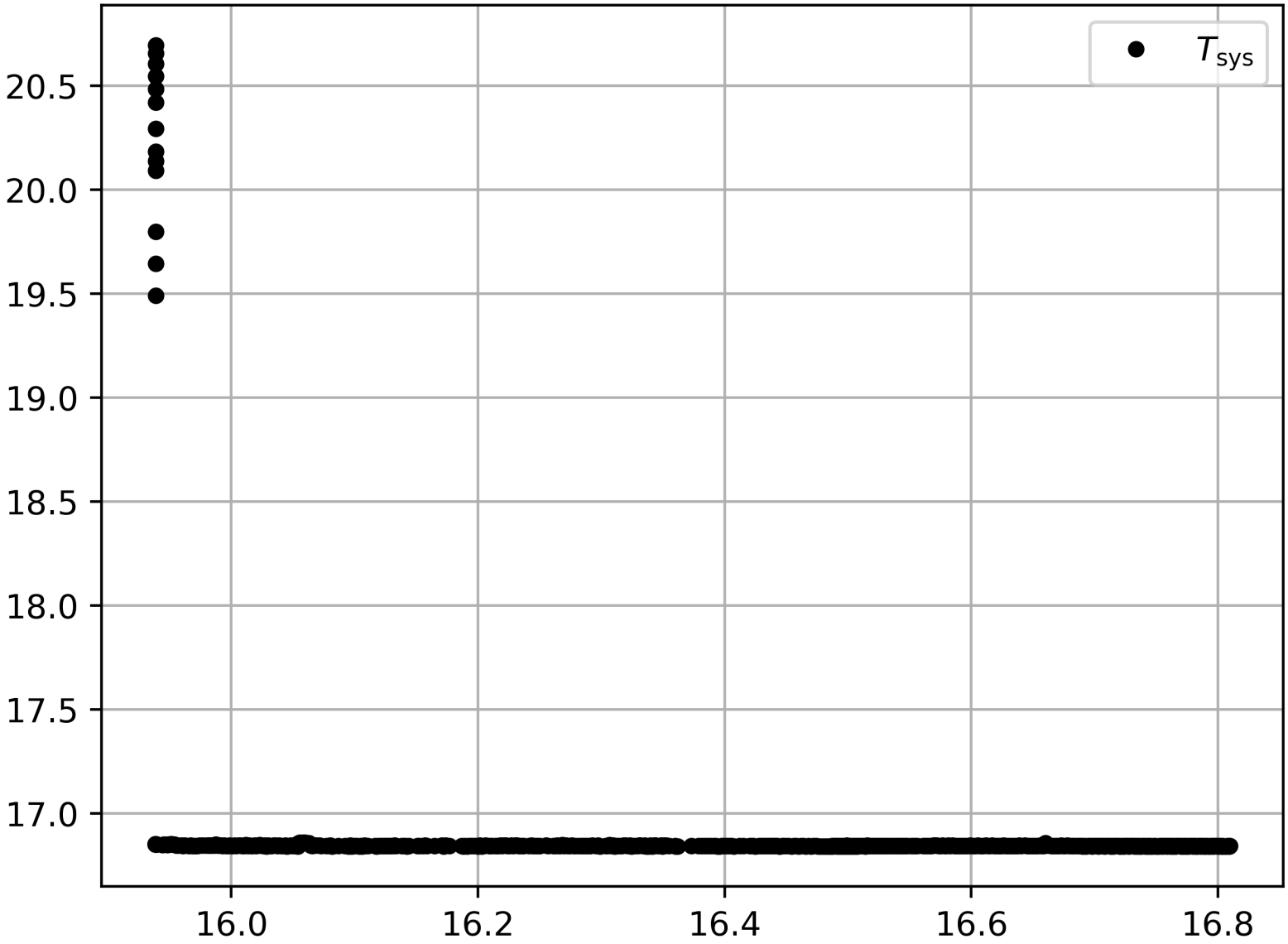


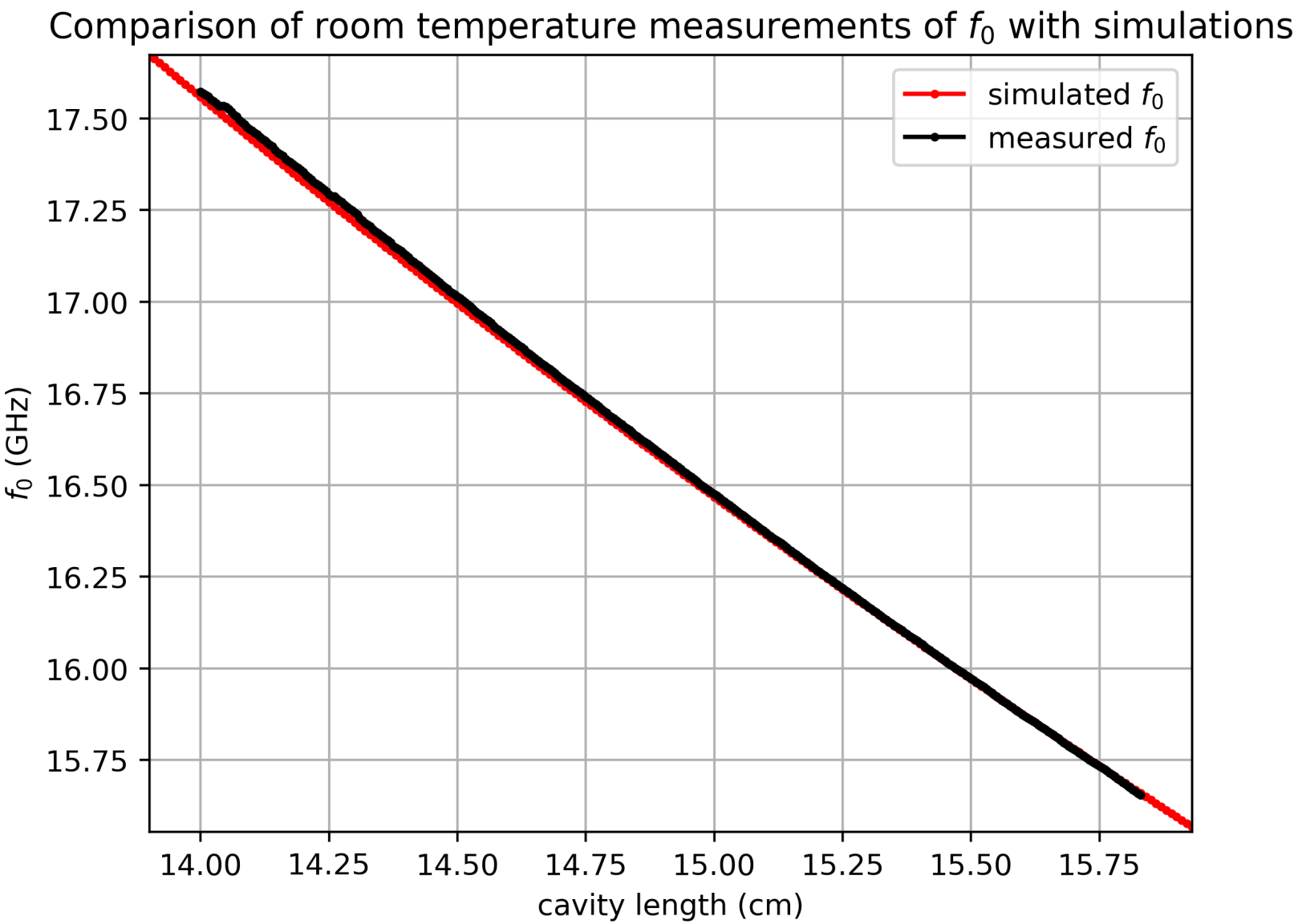

0.25
0.20
0.15
0.10
0.05
0.00
B [T]
Average Measured B field strength
07-31
08-01
10

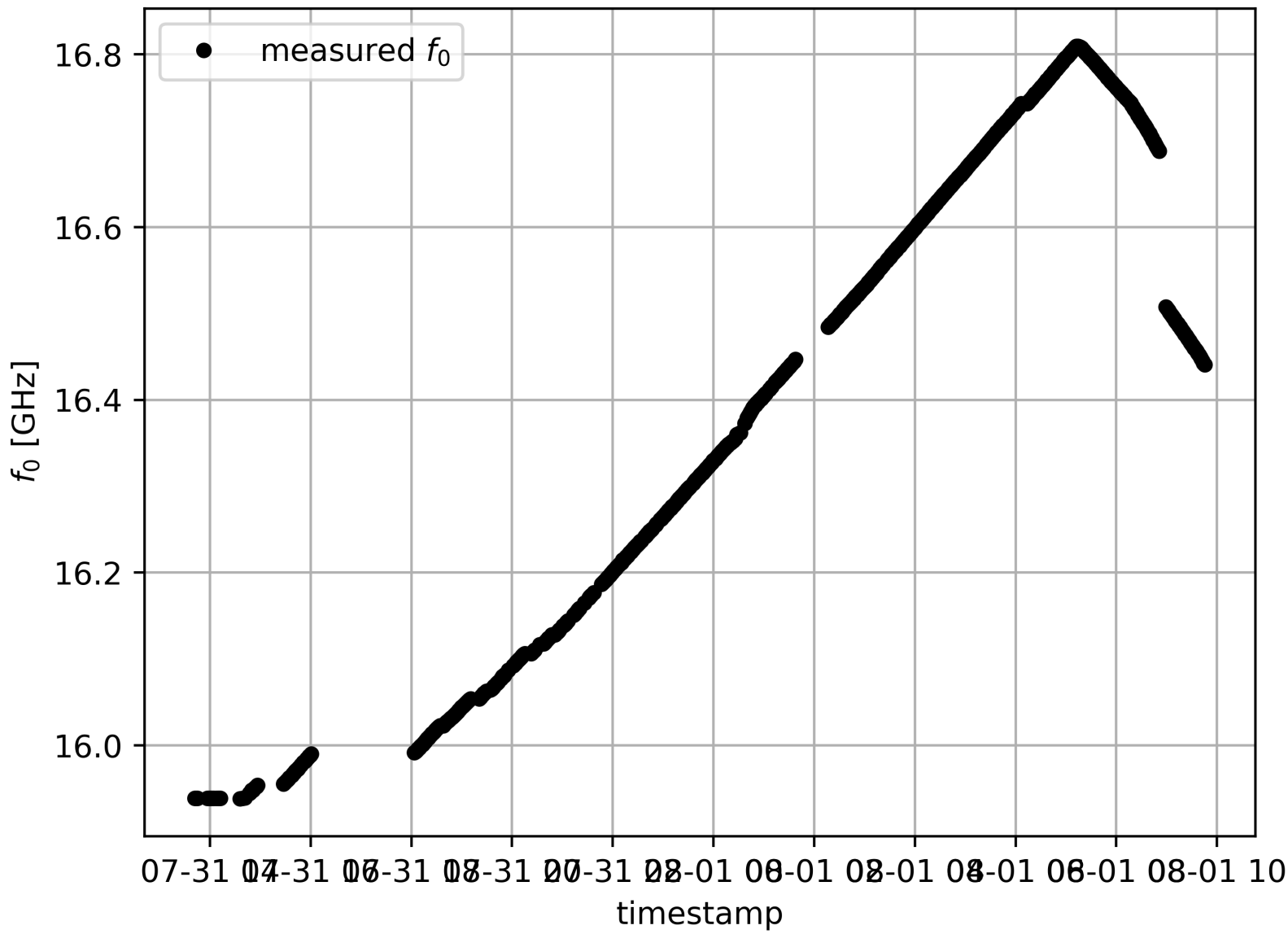

cryogenic LNA
amplifier mount
SMA-to-coax adaptor
through port
waveguide terminator
coupled port
strongly-coupled port
WR-62 crossguide coupler
2x scissor jacks
4x dielectric plate holders
curved mirror
weakly-coupled port (not drawn)
4x silver-coated guiding shafts
6x 1/4-20 threaded driving rods


β as a function of f_0
1.0
0.8
0.6
0.4
0.2
β
16.0
16.2
16.4
16.6
16.8
f_0 [GHz]


1e−21
7
6
5
4
3
2
1
0
$P_{\mathrm{sig}}(g_\gamma = 1)$ [W]
16.0
16.2
16.4
16.6
16.8
f_0 [GHz]


T_{sys}
20.5
20.0
19.5
19.0
18.5
18.0
17.5
17.0
16.0
16.2
16.4
16.6
16.8


Comparison of room temperature measurements of f_0 with simulations
simulated f_0
measured f_0
17.50
17.25
17.00
16.75
16.50
16.25
16.00
15.75
f_0 (GHz)
14.00
14.25
14.50
14.75
15.00
15.25
15.50
15.75
cavity length (cm)


measured f_0
16.8
16.6
16.4
16.2
16.0
f_0 [GHz]
07-31 14
07-31 16
07-31 18
07-31 20
07-31 22
08-01 00
08-01 02
08-01 04
08-01 06
08-01 08
08-01 10
timestamp